Eur. Phys. J. Special Topics **185**, 169–180 (2010)

DOI: 10.1140/epjst/e2010-01247-6

THE EUROPEAN PHYSICAL JOURNAL SPECIAL TOPICS

Regular Article

Vector rogue waves in binary mixtures of Bose-Einstein condensates

Yu.V. Bludov[1,a], V.V. Konotop[2,b], and N. Akhmediev[3,c]

[1] Centro de Física, Universidade do Minho, Campus de Gualtar, Braga 4710-057, Portugal
[2] Centro de Física Teórica e Computacional, Universidade de Lisboa, Avenida Professor Gama Pinto 2, Lisboa 1649-003, Portugal and Departamento de Física, Universidade de Lisboa, Campo Grande, Edifício C8, Piso 6, Lisboa 1749-016, Portugal
[3] Optical Sciences Group, Research School of Physics and Engineering, The Australian National University, Canberra ACT 0200, Australia

Received in final form and accepted 15 June 2010
Published online 23 August 2010

Abstract. We study numerically rogue waves in the two-component Bose-Einstein condensates which are described by the coupled set of two Gross-Pitaevskii equations with variable scattering lengths. We show that rogue wave solutions exist only for certain combinations of the nonlinear coefficients describing two-body interactions. We present the solutions for the combinations of these coefficients that admit the existence of rogue waves.

1 Introduction

Rogue waves [1,2] are waves occasionally appearing in the ocean that can reach the amplitudes more than twice the value of those in the surrounding chaotic wave field [3,4]. Above description can roughly be taken as the definition although variety of interpretations is still possible [5,6]. Being considered initially for ocean waves [7–10], nowadays the concept is shifted to other fields of physics, that can be modeled by similar nonlinear wave equations. Once the equations describing the phenomenon are established, understanding the features of rogue waves comes through finding special solutions that have the properties of having high amplitudes and are localized in space and in time [11,12]. From the experimental point of view it is much easier and safer to deal with rogue waves in a laboratory than in the open ocean. In addition to oceanic ones, rogue waves can be observed in variety of physical systems: optical fibers [13–15], arrays of optical waveguides [16], superfluids [17], capillary waves [18], and Bose-Einstein condensates (BEC) [19]. The latter system has the advantage that it admits variety of experimental conditions thus allowing for several types of rogue waves.

A remarkable feature of the BEC applications of the rogue waves is a possibility of experimental realization and observation of rogue waves in mixtures of several components which interact with each other. This could be spinor binary mixtures of atomic hyperfine states or condensates of atoms of different kinds: each type is nowadays routinely produced in many laboratories. Moreover, the inter-species interaction itself can originate modulational instability despite the fact that each component separately is modulationally stable (see e.g. [20]). Another significant advantage for modelling the rogue waves in BEC was already mentioned

[a] e-mail: bludov@fisica.uminho.pt
[b] e-mail: konotop@cii.fc.ul.pt
[c] e-mail: nna124@rsphymail.anu.edu.au

in [19]. Namely, it is the possibility of starting an experiment with perfectly stable system and switching it abruptly to an unstable state. The latter can be done with changing the sign of the scattering length by means of Fesbach resonance. This way we can control the nonlinearity in the governing Gross-Pitaevskii (GP) equation which is known beyond the BEC theory as nonlinear Schrödinger (NLS) equation. This unique possibility of preparation of the initial state for observation of rogue waves in a laboratory does not seem possible in any other physical system.

At this point we should clarify what in this paper is understood under the term *rogue wave*. We consider the deterministic phenomenon, i.e. the solutions that can be generated in the binary mixtures of BECs either by the phase and/or density engineering. These are solutions that emerge from the almost homogeneous background and disappear in a short interval of time, being followed by the developed instability pattern. Our rogue waves are characterised by the localised increase of the density amplitude several times above the unperturbed background. Mathematically, they correspond to the algebraic Peregrin's solutions and Akhmediev breathers [21–23] in the integrable limit. In our case, this limit is the Manakov set of equations [24].

In complex systems, we have to deal with several variables rather than a single wave amplitude. For example, considering the rogue waves in the financial world [26,27] as an example, we cannot restrict ourselves by only one variable – the amount of money. To describe the economy and its evolution in time, we have to take into account multiplicity of other forms money can take – shares, bonds and variety of other assets as well as all transformations between them. Clearly such complicated systems would describe the extreme waves with much higher accuracy than a single NLSE. Thus, our first task in modeling the rogue wave phenomenon is to consider the simplest models that still have more than one variable involved into the dynamics.

In this work, we study numerically the rogue waves in the two-component BECs which are described by the coupled set of two Gross-Pitaevskii (GP) equations with variable scattering lengths, i.e. coefficients of nonlinearity. Specifically, we present the rogue wave solutions for various combinations of these coefficients that admit such solutions. Among our major findings we can mention:

- Nontrivial relation between the existence of vector Peregrine solutions and the characteristics of the modulational instability of the system.
- Inhibition of the rogue waves due modulational stability induced by inter-atomic interaction
- Rogue waves induced by interatomic interactions in the mixture of condensates with positive scattering lengths (i.e. positive intra-atomic interactions)
- Rogue waves that are accompanied by the exchange of particles between the two components
- Possibility of existence of dark rogue waves.

The organization of the paper is as follows. In Sec. 2 we introduce the model and present some preliminary arguments of existence of vector rogue waves. In the subsequent sections 3 and 4 we present numerical studies of the rogues waves in the coupled GP equations without the linear coupling, i.e. without possibility of the conversion of the particles between the components and with such a possibility, respectively. The outcomes are summarized in Sec. 5.

2 The model and preliminary arguments

To be specific, we consider a spinor BEC composed of two hyperfine states, say of the $|F = 1, m_f = -1\rangle$ and $|F = 2, m_f = 1\rangle$ states of ^{87}Rb atoms [28] confined at different vertical positions by parabolic traps and coupled by a *time-dependent* coupling field.

We assume the condensate to be quasi-one-dimensional (cigar-shaped). Then, in the mean-field approximation the system is described by the GP equations [30,31]

$$i\frac{\partial\psi_1}{\partial t} = -\frac{\partial^2\psi_1}{\partial x^2} + \left(g_1|\psi_1|^2 + g|\psi_2|^2\right)\psi_1 + \beta(t)\psi_2, \tag{1a}$$

$$i\frac{\partial\psi_2}{\partial t} = -\frac{\partial^2\psi_2}{\partial x^2} + \left(g|\psi_1|^2 + g_2|\psi_2|^2\right)\psi_2 + \beta(t)\psi_1. \tag{1b}$$

Equation (1) are written in dimensionless form: the coordinate x and time t are measured in units of $\ell = \sqrt{\hbar/m\omega}$ and $2/\omega$, respectively, while the energies are measured in units of $\hbar\omega/2$, ω being the trap frequency in the (y,z)-plane. The dimensionless nonlinear coefficients, for the quasi-one-dimensional condensate, are given by $g_i \sim a_{ii}/a_{12}$. The coefficient of proportionality here depends on a particular choice of the transverse trap, and generally is either one or of the order of one. Therefore we do no specify it here. The factor g can take two values $g = \pm 1$ due to the fact that the dimensionless wavefunctions $\psi_{1,2}$ are measured in the units of $1/2\sqrt{|a_{12}|}$. The values $a_{ij} = a_{ji}$ are essentially the scattering lengths of inter-species (a_{12}) and intra-species (a_{ii}) in binary collisions. The last terms in Eq. (1) describe the possibility of conversion between the two hyperfine states, which can be originated by the external magnetic field. In this case, the factor β can be expressed in terms of such field. We emphasize that our results are not restricted to the described case. The model allows us for direct generalization to other binary mixtures consisting of spinor condensates [32,33] or of the condensates of atoms of two different kinds. In this last case one should set $\beta \equiv 0$.

To limit the number of possibilities, in the present work we deal only with the case where the intra-species interactions have the same signs of the scattering length, i.e. when $g_1 g_2 > 0$. We start some preliminary comments on the system (1), mentioning that an important parameter of the theory is the determinant of the nonlinear coefficients:

$$\Delta = g_1 g_2 - g^2 \tag{2}$$

which is known to determine the thermodynamic (see e.g. [31]) or modulational (see e.g. [20]) instability. In particular, one can distinguish the two degenerate cases as follows.

The first case is $\Delta = 0$ and $g g_{1,2} > 0$, i.e. the inter- and intra-species interactions all are either attractive or repulsive. Then Eq. (1) are reduced to the well known Manakov system [24], which we write down in the form

$$i\boldsymbol{u}_t = -\boldsymbol{u}_{xx} + g\boldsymbol{u}^\dagger \boldsymbol{u}\boldsymbol{u} \tag{3}$$

where $\boldsymbol{u} = \mathrm{col}(u_1, u_2)$. Eq. (3) naturally arises when $g_1 = g_2 = g$. Indeed, let us define the two matrices describing SU(2) rotations

$$\mathbf{R}_0 = \begin{pmatrix} \cos\alpha & \sin\alpha \\ -\sin\alpha & \cos\alpha \end{pmatrix} \qquad \text{and} \qquad \mathbf{R}_1 = \frac{1}{\sqrt{2}} \begin{pmatrix} e^{iB(t)} & -e^{-iB(t)} \\ e^{iB(t)} & e^{-iB(t)} \end{pmatrix} \tag{4}$$

where α is a real constant and the real function $B(t)$ is defined by $B(t) = -\int \beta(t)dt$. Then, defining also $\boldsymbol{\psi} = \boldsymbol{R}_1\boldsymbol{R}_0\boldsymbol{u}$ and taking into account that subject to this transformation the norm is invariant, i.e. $\boldsymbol{u}^\dagger\boldsymbol{u} = \boldsymbol{\psi}^\dagger\boldsymbol{\psi}$, from Eq. (3) we arrive at the evolution equation for the vector $\boldsymbol{\psi}$

$$i\boldsymbol{\psi}_t = -\boldsymbol{\psi}_{xx} + g\boldsymbol{\psi}^\dagger\boldsymbol{\psi}\boldsymbol{\psi} + \beta(t)\sigma_1\boldsymbol{\psi}. \tag{5}$$

Hereafter σ_j $(j = 1, 2, 3)$ are the standard Pauli matrixes.

Let us now suppose that we know a solution of Eq. (3), and more specifically, we choose it in a form of the "one-component" rogue wave [34]

$$\boldsymbol{u} = \Psi(x,t)\begin{pmatrix} 1 \\ 0 \end{pmatrix} \qquad \text{where } \Psi(x,t) \equiv \frac{1}{\sqrt{-g}}\left(1 - 4\frac{1+2it}{1+2x^2+4t^2}\right)e^{it} \tag{6}$$

which is valid for $g < 0$. This immediately leads to the one-parametric family of the rogue wave solutions of the system (5)

$$\boldsymbol{\psi} = \frac{1}{\sqrt{-2g}}\Psi(x,t)\begin{pmatrix} \cos\alpha e^{iB(t)} + \sin\alpha e^{-iB(t)} \\ \cos\alpha e^{iB(t)} - \sin\alpha e^{-iB(t)} \end{pmatrix}. \tag{7}$$

Another degenerate case corresponds to $\Delta = 0$ and $g g_{1,2} < 0$, i.e. scattering lengths of the inter- and intra-species interactions have different signs. Then for $\beta(t) \equiv 0$, Eqs. (1) are reduced to

the following set

$$i\frac{\partial w_1}{\partial t} = -\frac{\partial^2 w_1}{\partial x^2} + g\left(|w_1|^2 - |w_2|^2\right) w_1 \tag{8a}$$

$$i\frac{\partial w_2}{\partial t} = -\frac{\partial^2 w_2}{\partial x^2} + g\left(|w_2|^2 - |w_1|^2\right) w_2 \tag{8b}$$

More compact form of (8) in terms of $\mathbf{w} = \mathrm{col}(w_1, w_2)$ reads

$$i\mathbf{w}_t = -\mathbf{w}_{xx} + g(\mathbf{w}^\dagger \sigma_3 \mathbf{w})\sigma_3 \mathbf{w}. \tag{9}$$

Now we define the unitary matrixes

$$\mathbf{P}_0 = \begin{pmatrix} \cosh\alpha & \sinh\alpha \\ \sinh\alpha & \cosh\alpha \end{pmatrix} \qquad \text{and} \qquad \mathbf{P}_1 = \begin{pmatrix} \sinh\alpha & \cosh\alpha \\ \cosh\alpha & \sinh\alpha \end{pmatrix} \tag{10}$$

and introduce $\boldsymbol{\psi} = \mathbf{P}_j \boldsymbol{w}$. Then this $\boldsymbol{\psi}$ solves the system

$$i\frac{\partial \psi_1}{\partial t} = -\frac{\partial^2 \psi_1}{\partial x^2} + (-1)^j g\left(|\psi_1|^2 - |\psi_2|^2\right) \psi_1 \tag{11a}$$

$$i\frac{\partial \psi_2}{\partial t} = -\frac{\partial^2 \psi_2}{\partial x^2} + (-1)^j g\left(|\psi_1|^2 - |\psi_2|^2\right) \psi_2. \tag{11b}$$

It is clear that this case does not support vector rogue waves of the type $\psi_1 \sim \psi_2$, since by proper choice of the constant α in one of the matrices $\mathbf{P}_{0,1}$ one can reduce (11) to (8) with $|w_1|^2 = |w_2|^2$, which is a purely linear system. Below we will observe a signature of this "linearization" in the evolution of rogue waves in more general models.

3 Rogue waves in binary mixtures without linear coupling

Now we turn to nondegenrate situations, where $\Delta \neq 0$ and start with the case of the two components of the binary mixture without linear coupling. Thus, we take $\beta(t) \equiv 0$ in the general model (1). Clearly, one still can construct an analog of the solutions (7) (now with $\mathbf{R}_1 \equiv 1$) of Eqs. (1) in the form:

$$\psi_1(x,t) = a_1 \Psi(x,t), \quad \psi_2(x,t) = a_2 \Psi(x,t) e^{i\delta} \tag{12}$$

where $\Psi(x,t)$ is defined by (6), δ is a constant phase mismatch, and the amplitudes are given by the relations

$$a_1^2 = \frac{g - g_2}{\Delta}, \qquad a_2^2 = \frac{g - g_1}{\Delta}\ . \tag{13}$$

Since the solution (12) describes a synchronised evolution of the two components, we shall call it a *vector rogue wave*.

Usually, a rogue wave is located on an unstable background. Thus, we first seek for the conditions, when the background solution $(\psi_1^{(0)}, \psi_2^{(0)}) = (a_1, a_2)$ is unstable. To this end, we represent the solution of Eq. (1) in the form of a constant background a_j and a small excitation with the wavenumber k and the frequency ω. We suppose that its amplitude α_j, β_j is much smaller than the background $\alpha_j, \beta_j \ll a_j$ $(j = 1, 2)$:

$$\psi_j(x,t) = \left[a_j + \alpha_j \exp\left(ikx - i\omega t\right) + \bar{\beta}_j \exp\left(-ikx + i\omega t\right)\right] \exp\left[-i(g_j a_j^2 + g a_{3-j}^2)t\right]. \tag{14}$$

Substituting the solution in the form (14) into Eq. (1) and linearizing with respect to α_j, β_j, we obtain the dispersion relation in the long-wave limit (see, e.g., [20] for details)

$$\omega^2 = k^2 \left\{ g_1 a_1^2 + g_2 a_2^2 \pm \left[\left(g_1 a_1^2 + g_2 a_2^2\right)^2 - 4 a_1^2 a_2^2 \Delta\right]^{1/2} \right\}. \tag{15}$$

For the background to be unstable, Eq. (15) should have at least one imaginary root ω. It will occur when either of two conditions i) $g_{1,2} < 0$ or ii) $\Delta < 0$ is satisfied. All two-component rogue waves, described below, necessarily correspond to one of these cases.

Comparing (15) with (13) one readily concludes that the conditions for the existence of exact solutions in the form of the synchronised vector rogue waves are different from the conditions for the modulational instability of the background. In the Table 1, we analyse all possible situations for the cases where both types of the intra-species interactions have the same sign. To limit the number of cases here we have excluded the situations when $g_j < g < g_{3-j}$ with $j = 1, 2$. As it is clear, for $g_1 g_2 < 0$, the background is always unstable (now $\Delta < 0$).

Table 1. Occurrence of modulational instability and vector rogue waves for different relations among the parameters g characterizing inter- and intra-species interactions.

Intra-species interactions	Inter-species interactions	Unstable branches	Vector rogue wave
$g_{1,2} < 0$	$g < g_{1,2}$ $(\Delta < 0)$	1	does exist
	$\|g\| < \|g_{1,2}\|$ $(\Delta > 0)$	2	does exist
	$g > \|g_{1,2}\|$ $(\Delta < 0)$	1	does not exist
$g_{1,2} > 0$	$g < -g_{1,2}$ $(\Delta < 0)$	1	does exist
	$\|g\| < g_{1,2}$ $(\Delta > 0)$	stable	does not exist
	$g > g_{1,2}$ $(\Delta < 0)$	1	does not exist

3.1 Vector rogue waves

Let us first consider the situation when all two-body interactions are attractive, i.e. g, $g_{1,2} < 0$. Then it is possible to construct either the solution with $\Delta < 0$ (Fig. 1) or the solution with $\Delta > 0$, depicted in Fig. 2(a). In this case each of the components is modulationally unstable, provided the other component has zero density. As it is evident from Fig. 1(a), the initial conditions in the form of exact solution (12) indeed lead to the excitation of the two-component rogue wave. The two components reach their maximum values simultaneously, approximately at $t = 0$, and at the same location in the vicinity of $x = 0$. After reaching the maximum value, the rogue wave disappears at $t \approx 3$. The wave then returns back to the constant amplitude wave function. At a later stages of evolution ($t \approx 8$) the solution gains several chaotically located peaks due to the fact that the plane wave is modulationally unstable. Remarkably, these peaks appear simultaneously in the two components.

Now, after considering the exact solution (12) a natural question arises. How sensitive is the evolution with respect to the perturbations of the exact initial conditions given by Eq. (12). To answer this question, we performed simulations of Eq. (1) with initial conditions, when the two components are shifted relative to each other in comparison to the profiles given by Eq. (12). Specifically, the components have been shifted in opposite directions along the x-axis. Namely, $\psi_1(x,t) = a_1\Psi(x-1,t)$, $\psi_2(x,t) = a_2\Psi(x+1,t)$. Despite the initial shift, the components again reach their maxima simultaneously (see Fig. 1(b)) although at a later time $t \approx 0.25$ in comparison to the case of the exact solution. The coordinate of the maximum is also shifted to $x \approx -0.3$. This shift occurs due to the attraction of the weaker peak in the first component by the stronger one in the second component ($a_1 \approx 0.68$, $a_2 \approx 0.877$). Another notable difference is in the further evolution. Namely, the peaks arising due to the modulation instability appear at earlier times, $t \approx 4$, in comparison with the case reproducing the exact solution. Indeed, any destruction of the exact solution makes a contribution to perturbations that lead to modulation instability.

We also performed simulations using the initial conditions with the two components that are slightly different from the exact solution. Fig. 1(c) shows that the rogue wave in this case remains stable. The first peak in the evolution plot is very much similar to the ones in the two previous cases except for the location of the maximum of the first component ψ_1 which occurs at $t \approx -0.165$, while the maximum of the second component ψ_2 is reached at $t = -0.12$ i.e. earlier in comparison with the exact solution. However, the noise caused by modulation

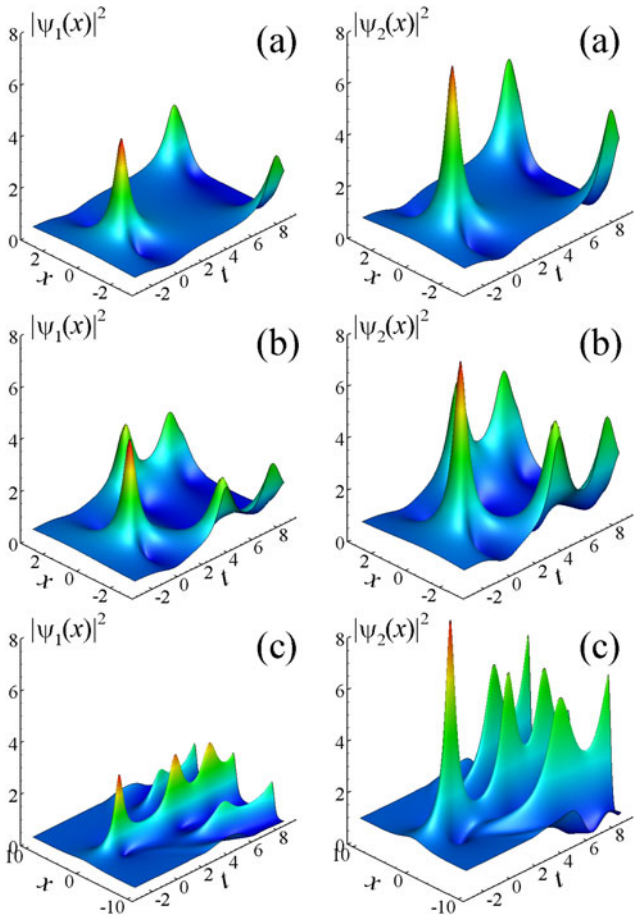

Fig. 1. (Color online) Vector rogue waves for the case when the parameters are $g_1 = -0.5$, $g_2 = -0.7$, $g = -1$ ($\Delta < 0$). The numerical simulations are performed for the initial conditions given by Eq. (12) with $\delta = 0$ at $t = -3$ [panels (a)]; with shifted maxima of the components along the x-axis: $\psi_1(x,t) = a_1\Psi(x-1,t)$, $\psi_2(x,t) = a_2\Psi(x+1,t)$ [panels (b)]; and with the detuned amplitudes of the coefficients: $\psi_1(x,t) = (a_1^2 - 0.3)^{1/2}\Psi(x,t)$, $\psi_2(x,t) = (a_2^2 + 0.3)^{1/2}\Psi(x,t)$ [panels (c)].

instability that appears at $t \gtrsim 3$ now is shifted from the sides of the numerical grid to the centre close to the point $x = 0$. We can also notice that the shape of these new peaks is similar to those for rogue waves although their amplitudes are lower.

Next we address the question of how the sign of the inter-species interactions influences the effect. To this end we hold all intra-species interactions attractive, require $\Delta > 0$, and change the sign of g. Typical results of these simulations are presented in Fig. 2. In each case, there are two unstable branches of the dispersion relation (see the Table 1) independent on the sign of inter-species interaction. However one observes rather different behaviour of the modes shown in the panels (a) and (b). In the case depicted in Fig. 2(a), attractive inter-species interactions result in smaller amplitudes of the vector rogue waves (see (13)) and the evolution is qualitatively similar to the one shown in Fig. 1(a). The latter is also obtained for all attractive interactions although in this case only one of the branches is unstable. Despite the large perturbation, the rogue wave survives and shows remarkable stability. The noise induced modulation instability appears at $t \approx 8$ i.e. at later stages of evolution similar to the case shown in Fig. 1(a). When, however we consider interspecies interactions to be repulsive ($g = 1$), the vector rogue wave requires much larger (compared to the case $g = -1$) initial amplitude. This results in significant increase of the growth rate for modulation instability. Thus, the modulation instability noise now appears right after the rogue wave (see Fig. 2(b)). The noise peaks have a structure different from the rogue wave itself. Namely, the minimum of one component is located at the point of

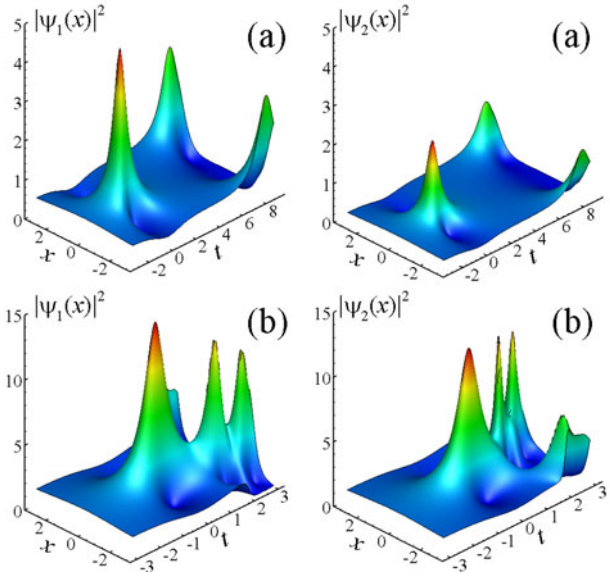

Fig. 2. (Color online) Vector rogue wave profiles when the parameters are: (a) $g_1 = -1.5$, $g_2 = -2.0$, $g = -1$ and (b) $g_1 = -1.5$, $g_2 = -2.0$, $g = 1$. In each case $\Delta > 0$. The initial conditions taken at $t = -3$ are the form of exact solutions (12) with $\delta = 0$. Thus, these are highly perturbed vector rogue waves.

the maximum of the other one and *vice versa*. This is not surprising if we recall the repulsive nature of the interspecies nonlinearity.

3.2 Vector rogue waves induced by the attractive interspecies interactions. Components with a positive and a negative scattering lengths

Now we turn our attention to the case when the rogue wave can exist in the component with a negative scattering length (we choose the first component, thus requiring $g_1 < 0$), but cannot exist in the other component with a positive scattering length (i.e. with $g_2 > 0$). A numerical example when this happens is shown in Fig. 3. Here $\Delta < 0$. It can be clearly seen from these numerical simulations that the rogue wave can now be excited, although there is a large difference in the amplitudes between the "driving" first component, which alone allows for the existence of the rogue waves, and the "driven" second component. The appearance of the rogue wave in the second component can be understood, if we take into account that $|\psi_2|^2 \ll |\psi_1|^2$ and neglect the density of the second component, $|\psi_2|^2$ in Eqs. (1). Then ψ_2 can be considered as a linear wave-function of the second component [see Eq. (1b)] in a trap potential $U = -|\psi_1|^2$ created by the first component. In other words, this is the vector rogue wave induced by the attractive inter-species interactions.

3.3 Nonexistence of rogue waves due to the strong inter-species interactions

Now we consider the case which is somehow opposite to the one considered in the previous subsection 3.2. Namely, we show that sufficiently strong inter-species interaction suppresses the existence of synchronised vector rogue waves, even though such waves can exist in each of the components separately. Thus, we consider the case when $g_{1,2} < 0$ and $g > |g_{1,2}|$ (again $\Delta < 0$).

What would be the physical mechanism responsible for this inhibition of vector rogue waves? In order to answer this question, we notice that this example emerges from the second case considered in Sec. 3.1 when Δ crosses zero point and the system is described by the model (8) [alternatively (9)]. Suppose, there is a vector solution, i.e. $w_2 = aw_1$, where a is a constant. Then for $|a| < 1$ (or $|a| > 1$), one can always find a constant α, $\tanh\alpha = a$ (or $\coth\alpha = a$)

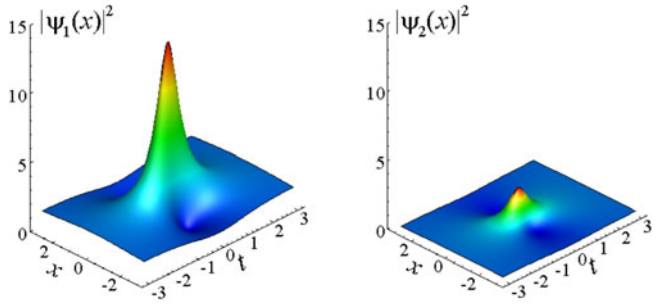

Fig. 3. (Color online) Vector rogue wave profiles when the parameters are $g_1 = -0.5$, $g_2 = 1.5$, $g = -1$ and the initial conditions taken at $t = -3$ are in the form of exact solutions (12) with $\delta = 0$.

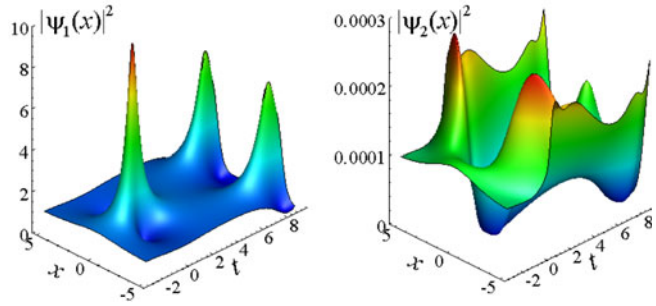

Fig. 4. (Color online) A vector rogue wave destroyed by the attractive interspecies interactions. Here $g_1 = g_2 = -0.95$, $g = 1$ and the initial conditions are taken at $t = -3$ in the form $\psi_1(x,t) = (-g_1)^{-1/2}\,\Psi(x,t)$, $\psi_2(x,t) = 0.01\;\Psi(x,t)$.

such that using one of the two matrices $\mathbf{P}_{1,2}$, defined in (10), we can arrive to $|\psi_1|^2 = |\psi_2|^2$. From here, we can see that the system displays pure linear dispersive dynamics. Indeed, the equations (11) become linear.

In order to confirm that this is indeed the case, we made numerical simulations using the initial condition in the form of the one-component rogue wave with slightly excited second component. The results of the simulation are depicted in Fig. 4. The excited state is an almost unperturbed rogue wave in the first component and a hole (or *dark rogue wave*) in the second component. The locations of their extremal points (maximum and minimum respectively) coincide. Clearly, the appearance of the dark rogue wave in the second component occurs due to the repulsive nature of the inter-species nonlinearity. Indeed, neglecting much smaller density values of the second component in Eq. (1b) we arrive at the linear Schrödinger equation with the shape of the potential created by the first component. Contrary to the case considered in Sec. 3.3 and depicted in Fig. 3, the potential has the opposite sign thus creating the potential barrier for the second component.

The centre of the rogue wave does not have to be at the point $t = 0$. Indeed, the rogue wave in Fig. 4 is excited earlier in time. Additional structures that appear as noise in this plot, namely, lateral maxima of the second component (at $t \approx 0.5$ and $x \approx \pm 3.85$) are not synchronised with the structures (lateral maxima at $t = 0$ and $x \approx \pm 1.2$) in the first component. This fact is also in agreement with our physical understanding of this case.

3.4 Rogue waves induced by the attractive interspecies interactions. Components with positive scattering lengths

Quite an opposite situation occurs in the case $g_{1,2} > 0$, $g < 0$, and $\Delta < 0$. No rogue waves can exist in each of the components separately. However, the favorable conditions for rogue waves are created due to inter-species interactions. Rogue waves in this case are even more pronounced than in the case considered above in Sec. 3.2. The rogue wave profiles calculated

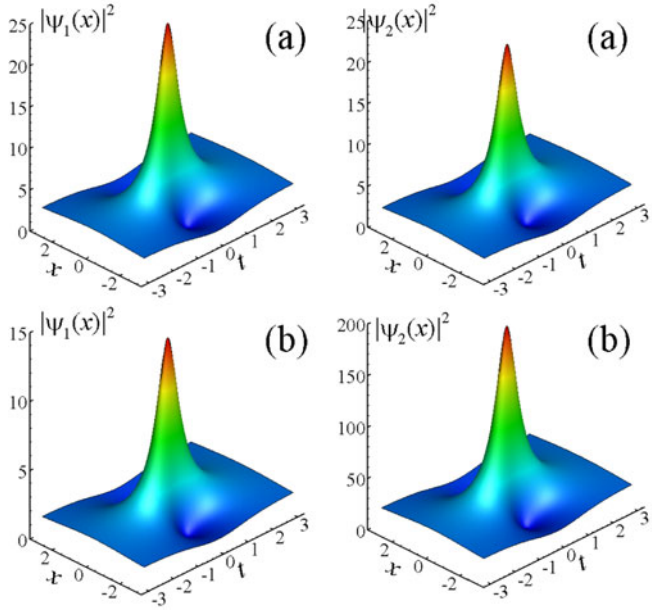

Fig. 5. (Color online) Two-component rogue wave profiles in the system with the parameters (a) $g_1 = 0.5$, $g_2 = 0.7$, $g = -1$ and (b) $g_1 = 13.0$, $g_2 = 0.025$, $g = -1$. The initial conditions for these simulations are taken at $t = -3$ in the form of exact solutions Eq. (12) with $\delta = 0$. Note the difference in scales along vertical axis in (b).

for two different combinations of $g_{1,2}$ are shown in Fig. 5. In the first case (Fig. 5(a)), the two BEC components have approximately equal amplitudes while in the second case (Fig. 5(b)), the two BEC components differ significantly in the amplitude. In each case, the attractive interspecies nonlinearity g creates conditions for existence of stable vector rogue waves with the two nonzero components.

4 Rogue waves in binary mixtures with linear coupling

The system becomes physically significantly different when we take into account time-dependent linear coupling $\beta(t) \neq 0$ in Eq. (1). This term is responsible for the particle exchange between the two components. The number of particles in the first and in the second components relative to the total number of particles can be expressed using Eq. (7) as

$$\frac{\int |\psi_{1,2}(x)|^2 dx}{\int |\Psi(x)|^2 dx} = -\frac{1}{2g}\left[1 \pm \sin(2\alpha)\cos(2B(t))\right], \tag{16}$$

where the signs + and − in the right hand side correspond to the first and the second components, respectively. As it follows from Eq. (16), when $\alpha = \pi/4 + n\pi/2$ with n being an integer, it is possible that all particles are concentrated in one of the components. Moreover, if we choose the linear dependence of the phase $B(t)$ on time

$$B(t) = \frac{\pi}{4}\left[1 - b\frac{t - t_0}{t_0}\right] \tag{17}$$

the particles are periodically swapped between the two components. In the following discussion we concentrate on this case only.

Fig. 6 shows the results of numerical simulations of vector rogue waves in BECs with linear coupling. The values of parameters chosen for these simulations are given in the figure caption. In the first case, $b = 1$, shown in Fig. 6(a), the maximum of the rogue wave is located at the

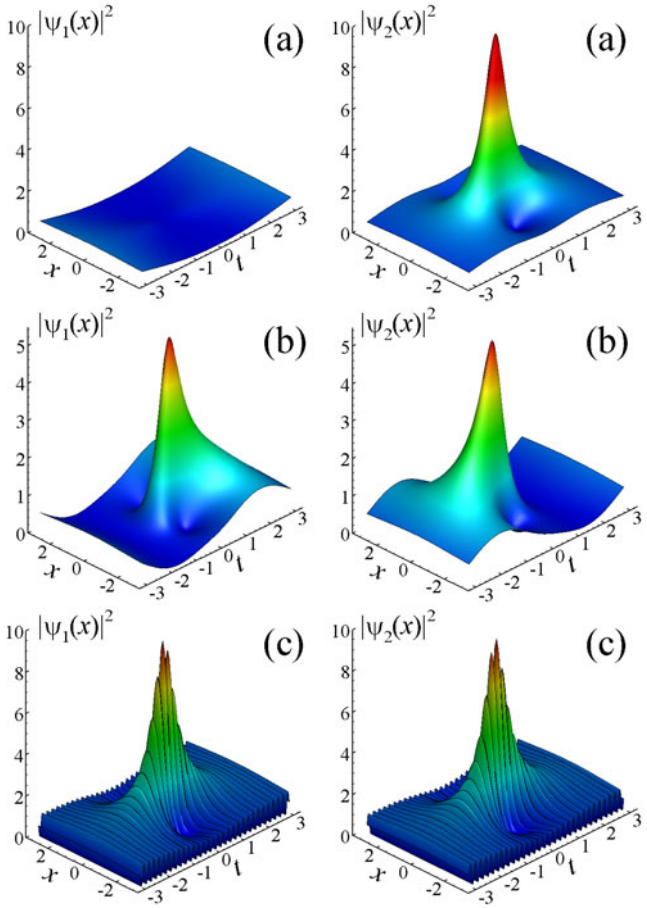

Fig. 6. (Color online) Vector rogue wave profiles for the case $g_{1,2} = g = -1$, $\alpha = \pi/4$, $t_0 = -3$, and linear coupling (17) with (a) $b = 1$, (b) $b = 2$ and (c) $b = 15$.

maximum of the oscillating background. All particles at $t = 0$ are concentrated in the second component. In the second case, $b = 2$, shown in Fig. 6(b), the maximum of the rogue wave is located at the slope of the oscillating background. There is an equal number of particles in the two components. The slope in the background results in the shift in time between the location of maxima of the two components ($t \approx 0.154$ in first component and $t \approx -0.154$ in second component). Finally, when the frequency of the oscillation of the particles between the two components is high ($b = 15$), the background becomes fast oscillating as can be seen in Fig. 6(c). Despite the fast oscillations, the shape of the rogue wave components in average is little influenced by them.

5 Discussions

In this work, we showed that BEC is a perfect system that allows us to study two-component rogue waves and the effect of nonlinear interactions on their dynamics. We have shown that there is a diversity of vector rogue waves in coupled systems. The possibility of external control of the interaction coefficients adds flexibility in our ability to switch between various rogue wave appearances when we want it. Moreover, when the linear interspecies interactions are added, their variation appears to be an effective tool for manipulating vector rogue waves, thus, allowing us to observe many different scenarios.

Adding to discussions suggested by the editors of this special issue we can say that appearance of vector rogue waves in this problem is naturally related to modulation instability.

As soon as modulation instability is turned on, the rogue wave solution also appears as a result. This may be a specific feature of this model as it is a natural extension of the NLS equation. However, some kind of instability is a necessary condition for appearance of rogue waves provided that the model itself is nonlinear. Clearly, in any linear problem, rogue wave is just the result of the constructive wave interference [35] rather than growth of instability. The phenomenon observed in [35] is more related to Anderson localisation than to rogue waves.

Our study is only the first step in exploring rogue waves in mixtures of condensed quantum gases. Advanced analytical description of the phenomenon will allow us to solve more complicated problems. We can mention, in this respect, evolution of rogue waves in variety of trapping potentials. These may include a parabolic trap or an optical lattice. First studies in this direction performed with the one-component Bose-Einstein condensate were done in [19]. We can also mention vector rogue waves in more than one dimension. We can take into account quantum fluctuations which are expected to be enhanced when a rogue wave achieves its maximum. Another possibility is managing rogue waves by means of time and/or space dependent external forces.

We can consider two-component Bose-Einstein condensate as a first step to generalisations of the simple one component model. Multi-component dynamical systems are naturally occurring in the complex world surrounding us. They may appear in biology when considering several interacting species or in the world of finance [36]. Depending on the particular situation, perhaps, we would like to avoid any extreme events or disasters. The problem that we solved, allows us to make the first steps in the direction of controlling such complicated systems using interactions between the components. For example, wouldn't it be nice to prevent catastrophes in economy just controlling transformations between various forms the money can take? Indeed, controlling the interactions seems to be the simplest way of governing the complicated world of finances. The problem that we solved here can be considered as the first step in this direction. Further understanding of extreme events (rogue waves) is the natural way to make the world we are living in to be better.

V.V.K. acknowledges warm hospitality of the Laboratoire de Physique des Lasers, Atoms e Molécules at Université des Sciences et Technologies de Lille where a part of the work was done. The work of V.V.K. was partially supported by the Université de Lille I. The work of N.A. is supported by the Australian Research Council (Discovery Project DP0985394).

References

1. C. Garrett, J. Gemmrich, Physics Today **62** (2009)
2. P. Müller, Ch. Garrett, A. Osborne, Oceanography **18**, 66 (2005)
3. K. Dysthe, H.E. Krogstad, P. Müller, Annu. Rev. Fluid Mech. **40**, 287310 (2008)
4. W. Rosenthal, S.Lehner, H. Dankert, H. Guenther, K. Hessner, J. Horstmann, A. Niedermeier, J.C. Nieto-Borge, J. Schulz-Stellenfleth, K. Reichert, *Proceedings of MAXWAVE Final Meeting October 8–10* (Geneva, Switzerland, 2003)
5. C. Kharif, E. Pelinovsky, European J. Mech. B (Fluids) **22**, 603 (2003)
6. A.R. Osborne, Marine Structures **14**, 275 (2001)
7. C. Kharif, E. Pelinovsky, A. Slunyaev, *Rogue waves in the ocean* (Springer, Heidelberg, 2009)
8. A.R. Osborne, *Nonlinear ocean waves* (Academic Press, 2009)
9. P.A.E.M. Janssen, J. Physical Oceanography **33**, 863 (2003)
10. A.R. Osborne, M. Onorato, M. Serio, Phys. Lett. A **275**, 386 (2000)
11. N. Akhmediev, J.M. Soto-Crespo, A. Ankiewicz, Phys. Lett. A **373**, 2137 (2009)
12. N. Akhmediev, A. Ankiewicz, M. Taki, Phys. Lett. A **373**, 675 (2009)
13. D.R. Solli, C. Ropers, P. Koonath, B. Jalali, Nature **450**, 1054 (2007)
14. D.-I. Yeom, B. Eggleton, Nature **450**, 953 (2007)
15. G. Genty, C.M. de Sterke, O. Bang, F. Dias, N. Akhmediev, J.M. Dudley, Phys. Lett. A **374**, 989 (2010)
16. Yu.V. Bludov, V.V. Konotop, N. Akhmediev, Opt. Lett. **34**, 3015 (2009)
17. A.N. Ganshin, V.B. Efimov, G.V. Kolmakov, L.P. Mezhov-Deglin, P.V.E. McClintock, Phys. Rev. Lett. **101**, 065303 (2008)

18. M. Shatz, H. Punzmann, H. Xia, Capillary rogue waves, Phys. Rev. Lett. **104**, 104503 (2010)
19. Yu.V. Bludov, V.V. Konotop, N. Akhmediev, Phys. Rev. A **80**, 033610 (2009)
20. N.A. Kostov, V.Z. Enolskii, V.S. Gerdjikov, V.V. Konotop, M. Salerno, Phys. Rev. E **70**, 056617 (2004)
21. K.B. Dysthe, K. Trulsen, Phys. Scr. **T82**, 48 (1999)
22. V.V. Voronovich, V.I. Shrira, G. Thomas, J. Fluid Mech. **604**, 263 (2008)
23. P.K. Shukla, et al., Phys. Rev. Lett. **97**, 094501 (2006)
24. S.V. Manakov, Zh. Eksp. Teor. Fiz. **67**, 543 (1974)
25. S.V. Manakov, Sov. Phys. JETP **38**, 248 (1974)
26. `http://www.financialsense.com/series2/rogue2.html`
27. Z. Yan, Financial rogue waves [`arXiv:0911.4251`] (2009) (preprint)
28. M.R. Matthews, et al., Phys. Rev. Lett. **83**, 3358 (1999)
29. J. Williams, et al., Phys. Rev. A **61**, 033612 (2000)
30. L. Pitaevskii, S. Stringari, *Bose-Einstein Condensation* (Oxford University Press, 2003)
31. C.J. Pethick, H. Smith, *Bose-Einstein Condensation in Dilute Gases* (Cambridge University Press, Cambridge, UK, 2002)
32. P. Maddaloni, et al., Phys. Rev. Lett. **85**, 2413 (2000)
33. F. Minardi, et al., Phys. Rev. Lett. **87**, 2498 (2001)
34. D.H. Peregrine, J. Austral. Math. Soc., Ser B **25**, 16 (1983)
35. R. Höhmann, U. Kuhl, H.-J. Stöckmann, L. Kaplan, E.J. Heller, Phys. Rev. Lett. **104**, 093901 (2010)
36. V.M. Yakovenko, J.B. Rosser Jr., Rev. Mod. Phys. **81**, 1703 (2009)